

Measurement of the ${}^3\text{He}(e, e'p)pn$ reaction at high missing energies and momenta

F. Benmokhtar,^{1,2} M. M. Rvachev,³ E. Penel-Nottaris,⁴ K. A. Aniol,⁵ W. Bertozzi,³ W. U. Boeglin,⁶ F. Butaru,⁴ J. R. Calarco,⁷ Z. Chai,³ C. C. Chang,⁸ J. -P. Chen,⁹ E. Chudakov,⁹ E. Cisbani,¹⁰ A. Cochran,¹¹ J. Cornejo,⁵ S. Dieterich,¹ P. Djawotho,¹² W. Duran,⁵ M. B. Epstein,⁵ J. M. Finn,¹² K. G. Fissum,¹³ A. Frahi-Amroun,² S. Frullani,¹⁰ C. Furget,⁴ F. Garibaldi,¹⁰ O. Gayou,¹² S. Gilad,³ R. Gilman,^{1,9} C. Glashauser,¹ J.-O. Hansen,⁹ D. W. Higinbotham,^{3,9} A. Hotta,¹⁴ B. Hu,¹¹ M. Iodice,¹⁰ R. Iomni,¹⁰ C. W. de Jager,⁹ X. Jiang,¹ M. K. Jones,^{9,8} J. J. Kelly,⁸ S. Kox,⁴ M. Kuss,⁹ J. M. Laget,¹⁵ R. De Leo,¹⁶ J. J. LeRose,⁹ E. Liatard,⁴ R. Lindgren,¹⁷ N. Liyanage,⁹ R. W. Lourie,¹⁸ S. Malov,¹ D. J. Margaziotis,⁵ P. Markowitz,⁶ F. Merchez,⁴ R. Michaels,⁹ J. Mitchell,⁹ J. Mougey,⁴ C. F. Perdrisat,¹² V. A. Punjabi,¹⁹ G. Quémener,⁴ R. D. Ransome,¹ J.-S. Réal,⁴ R. Roché,²⁰ F. Sabatié,²¹ A. Saha,⁹ D. Simon,²¹ S. Strauch,¹ R. Suleiman,³ T. Tamae,²² J. A. Templon,²³ R. Tieulent,⁴ H. Ueno,²⁴ P. E. Ulmer,²¹ G. M. Urciuoli,¹⁰ E. Voutier,⁴ K. Wijesooriya,²⁵ and B. Wojtsekhowski⁹

(The Jefferson Lab Hall A Collaboration)

¹Rutgers, The State University of New Jersey, Piscataway, New Jersey 08854, USA

²Université des Sciences et de la Technologie, BP 32, El Alia, Bab Ezzouar, 16111 Alger, Algérie

³Massachusetts Institute of Technology, Cambridge, Massachusetts 02139, USA

⁴Laboratoire de Physique Subatomique et de Cosmologie, F-38026 Grenoble, France

⁵California State University, Los Angeles, Los Angeles, California 90032, USA

⁶Florida International University, Miami, Florida 33199, USA

⁷University of New Hampshire, Durham, New Hampshire 03824, USA

⁸University of Maryland, College Park, Maryland 20742, USA

⁹Thomas Jefferson National Accelerator Facility, Newport News, Virginia 23606, USA

¹⁰INFN, Sezione Sanità and Istituto Superiore di Sanità, Laboratorio di Fisica, I-00161 Rome, Italy

¹¹Hampton University, Hampton, Virginia 23668, USA

¹²College of William and Mary, Williamsburg, Virginia 23187, USA

¹³University of Lund, Box 118, SE-221 00 Lund, Sweden

¹⁴University of Massachusetts, Amherst, Massachusetts 01003, USA

¹⁵CEA-Saclay, F-91191 Gif Sur-Yvette Cedex, France

¹⁶INFN, Sezione di Bari and University of Bari, I-70126 Bari, Italy

¹⁷University of Virginia, Charlottesville, Virginia 22901, USA

¹⁸State University of New York at Stony Brook, Stony Brook, New York 11794, USA

¹⁹Norfolk State University, Norfolk, Virginia 23504, USA

²⁰Florida State University, Tallahassee, Florida 32306, USA

²¹Old Dominion University, Norfolk, Virginia 23529, USA

²²Laboratory of Nuclear Science, Tohoku University, Sendai 982-0826, Japan

²³University of Georgia, Athens, Georgia 30602, USA

²⁴Yamagata University, Kojirakawa-machi 1-4-12, Yamagata 990-8560, Japan

²⁵University of Illinois, Champaign-Urbana, Illinois 61801, USA

(Dated: August 17, 2004)

Results of the Jefferson Lab Hall A quasielastic ${}^3\text{He}(e, e'p)pn$ measurements are presented. These measurements were performed at fixed transferred momentum and energy, $q = 1502$ MeV/c and $\omega = 840$ MeV, respectively, for missing momenta p_m up to 1 GeV/c and missing energies in the continuum region, up to pion threshold; this kinematic coverage is much more extensive than that of any previous experiment. The cross section data are presented along with the effective momentum density distribution and compared to theoretical models.

PACS numbers: 25.30.Fj, 27.10.+h

The single-particle properties of nuclei have been extensively studied, in particular through inclusive (e, e') and coincidence $(e, e'p)$ reactions, leading to strong constraints on nuclear structure models and a good understanding of the one-body properties of nuclei. An improved understanding of nuclei beyond the one-body properties is now one of the major goals of nuclear physics. Exclusive $(e, e'p)$ measurements for example can provide information on the spatial structure of nuclei at a resolution less than the size of the nucleons, where corre-

lations between two or more nucleons are expected to be significant. By choosing appropriate kinematics one can enhance the effects of nucleon-nucleon correlations relative to the effects of final-state interactions (FSI) and other reaction-mechanism effects. Understanding correlations, particularly short-range correlations, might require consideration of the underlying quark substructure of the nucleon. In this letter we present a study of NN correlations in ${}^3\text{He}$ with the $(e, e'p)pn$ reaction.

First we present two signatures of NN correlations in

${}^3\text{He}$ that one might expect to observe in the $(e, e'p)$ reaction. Consider an electron which scatters on a proton belonging to a pair of correlated nucleons inside a nucleus, ${}^3\text{He}$ in our case [1, 2], transferring energy ω and momentum \vec{q} . In the center of mass system of the two nucleons, these nucleons will have equal and opposite momenta, $\pm\vec{p}_m$, which will be large if they are close together. In the plane-wave impulse approximation (PWIA) - see Fig. 1a - the interaction between the outgoing nucleon and the residual nuclear fragments is neglected. If we further neglect the momentum of the pair relative to the residual nucleus (here a single nucleon), the struck proton is ejected with momentum $\vec{q} - \vec{p}_m$, while the other nucleon of the pair moves off with the recoil momentum of the reaction, \vec{p}_m . The spectator nucleon is at rest, so this is the three-body breakup (3bbu) reaction channel, as opposed to the two-body breakup (2bbu) channel with a pd final state. The spectator nucleon and the undetected nucleon of the pair constitute a recoil system of mass:

$$M_r^2 = \left[M_{A-2} + \sqrt{M_N^2 + p_m^2} \right]^2 - p_m^2. \quad (1)$$

Here M_N is the mass of the detected nucleon and M_{A-2} is the mass of the $A - 2$ nuclear system.

Thus, in PWIA, a signature of the disintegration of correlated nucleons is the appearance of a peak in the cross section as a function of missing energy, E_m , in the continuum region, with the position depending on p_m : $E_m = M_r + M_p - M_A$. The correlation peak was observed for the first time at Saclay [3]. The peak width reflects the motion of the center of mass with respect to the spectator nucleon and its magnitude is directly related to the wave function of the two correlated nucleons. The peak thus signifies the absorption of virtual photons on nucleons correlated in pairs, as in the electro-disintegration of deuterons. This picture remains valid even if the two nucleons of the correlated pair reinteract - see Fig. 1b.

In PWIA, the integral over the continuum gives the momentum distribution of the proton in the pair. The integral is obtained experimentally by dividing the experimental cross section by the elementary off-shell electron-proton cross section σ_{ep} [4] multiplied by a kinematic factor K , and integrating over missing energy:

$$\eta(p_m) = \int \left(\frac{d^6\sigma}{dE_e dE_p d\Omega_e d\Omega_p} / K \sigma_{ep} \right) dE_m. \quad (2)$$

The momentum distribution will yield a second signature of NN correlations. One might expect that NN correlations lead preferentially to 3bbu rather than 2bbu, due to the reduced probability for the two undetected nucleons to form a bound deuteron. Thus, the signature is that as NN correlations become important at missing momenta greater than the Fermi momentum, the momentum distribution from 3bbu will be enhanced relative to that for 2bbu.

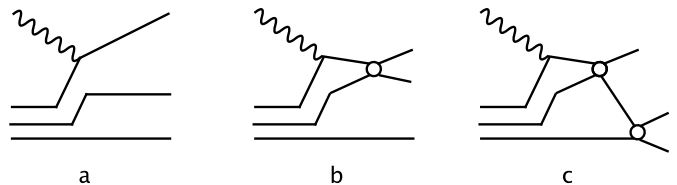


FIG. 1: Feynman diagrams for a) PWIA, b) rescattering, and c) rescattering with the spectator nucleon.

This simple picture is complicated by several factors, so that data must be compared to detailed calculations before drawing conclusions about NN correlations in nuclei. First, the peak in the missing energy has a purely kinematic origin, in that it will appear as long as the ${}^3\text{He}$ electrodisintegration involves two active nucleons plus a spectator nucleon. Second, the effective momentum density distribution is an actual density only in the PWIA limit. This picture is modified by final-state interactions and meson-exchange currents (MEC). When the two nucleons in the active pair rescatter, the position and width of the peak do not change; but one measures the transition between a correlated pair in the ground state and a correlated pair in the continuum. When one of the nucleons of the active pair reinteracts with the spectator third nucleon - see Fig. 1c - the position, shape, and amplitude of the peak might all be affected.

In Thomas Jefferson National Accelerator Facility (JLab) Hall A experiment E89-044 [5], we studied the ${}^3\text{He}(e, e'p)$ reaction in the quasielastic region at transferred 3-momentum $|\vec{q}| = 1502$ MeV/ c and energy $\omega = 840$ MeV, so $Q^2 = 1.55$ GeV 2 . This paper reports the results of measurements in perpendicular kinematics with Bjorken $x = 0.98$, near the top of the quasifree peak. Protons were detected at several angles relative to \vec{q} , corresponding to missing momenta p_m of 0 - 1 GeV/ c . Results of the 2bbu channel ${}^3\text{He}(e, e'p)d$ from this experiment were reported in [6]; here we focus on the continuum ${}^3\text{He}(e, e'p)pn$ channel, $E_m > 7.72$ MeV.

A continuous, ~ 120 μA , electron beam was scattered from ${}^3\text{He}$ in a 10 cm diameter cylindrical cell, mounted with the beam passing through the center of the target perpendicular to the symmetry axis. The ${}^3\text{He}$ target density was ~ 0.072 g/cm 3 [6]. The scattered electrons and knocked-out protons were detected in the two High-Resolution Spectrometers (HRS $_e$ and HRS $_h$). Details of the Hall A experimental setup are given in [7].

Throughout the experiment, singles ${}^3\text{He}(e, e')$ quasielastic scattering data, measured simultaneously with coincidence ${}^3\text{He}(e, e'p)$, provided a continuous monitor of both luminosity and beam energy. The absolute normalization of our data was determined by comparing measurements of elastic scattering data to

TABLE I: Proton spectrometer kinematic settings.

p_m (MeV/c)	P_p (MeV/c)	θ_p ($^\circ$)
150	1493	54.04
300	1472	59.83
425	1444	64.76
550	1406	69.80
750	1327	78.28
1000	1171	89.95

world data [8]. We measured the ${}^3\text{He}(e, e'p)X$ cross section at three beam energies, keeping $|\vec{q}|$ and ω fixed in order to separate response functions and understand systematic uncertainties. The data reported in this paper were all obtained at a beam energy of 4806 MeV.

The missing energy resolution, about 1 MeV FWHM, is less than the 2.23 MeV separation between the ${}^3\text{He}(e, e'p)d$ peak and the threshold for the ${}^3\text{He}(e, e'p)pn$ breakup channels. The radiative corrections to the measured cross sections were performed by using the code MCEEP [9]. The radiative tail is simulated and folded into the (E_m, p_m) space based on the prescription of Borie and Drechsel [10]. The radiative corrections in the continuum amount to 10 – 20% of the cross section. In particular, the radiative corrections remove the tail of the 2bbu process from the 3bbu data, allowing a clear separation of the channels.

Table I shows the central proton spectrometer settings for the experimental kinematics analyzed for this paper. These 6 settings are divided into numerous (E_m, p_m) bins for presentation; Fig. 2 shows the radiatively corrected cross section as a function of missing energy for several selected bins. The energy scale in the horizontal axis has been shifted in these plots so that the 3bbu channel starts at 0. As p_m increases, we can see that the broad peak in the cross section moves to higher missing energies. The arrow in the figure indicates where one would expect the peak in the cross section due to the photon coupling to a nucleon in a correlated pair at rest inside the ${}^3\text{He}$ nucleus; the expected peak position for $p_m = 820$ MeV/c is just off scale, at $E_m \approx 145$ MeV. The close correspondence of the peak in the data with the arrow indicates the importance of two-nucleon processes such as correlations. The peak width reflects the motion of the center of mass of the correlated pair.

Several calculations are presented in Fig. 2. The simplest calculation is a PWIA calculation using Salme's spectral function [11] and the σ_{cc1} electron-proton off-shell cross section [4]. Also shown in Fig. 2 are the results of microscopic calculations of the continuum cross section by J. M. Laget [12], including a plane-wave impulse approximation, and successive implementation of

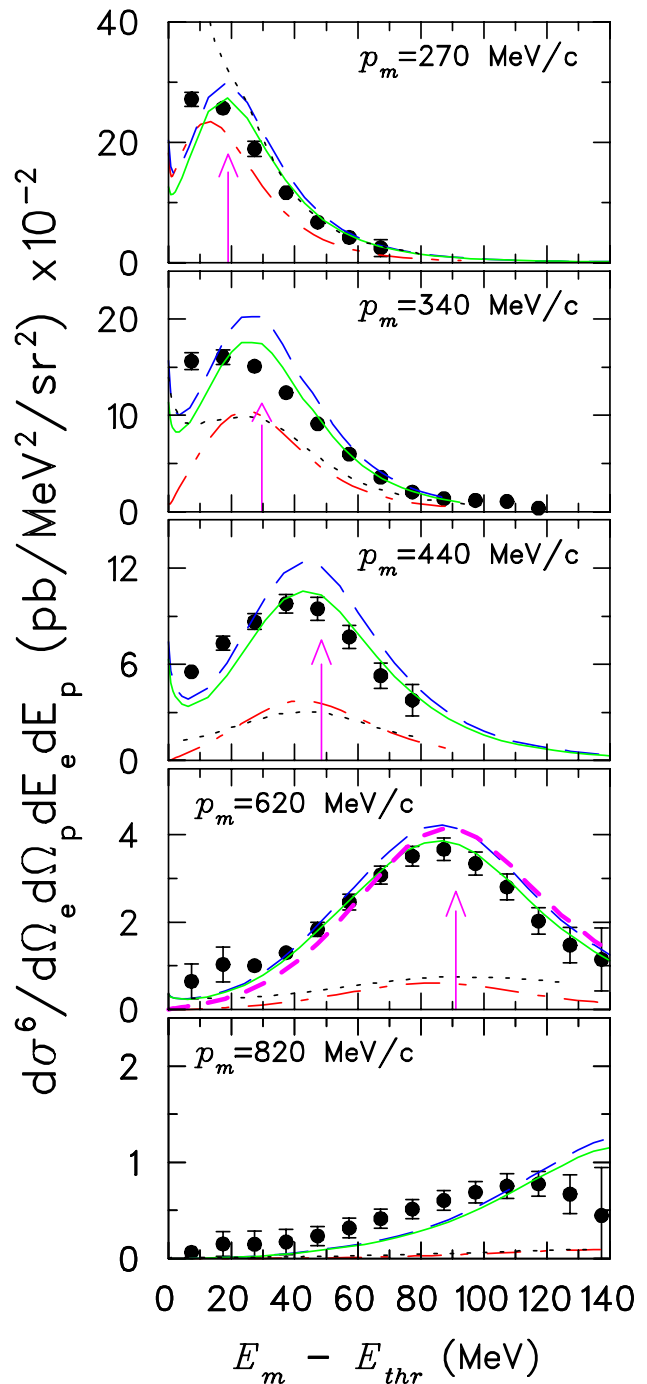


FIG. 2: (color online). Cross-section results for the ${}^3\text{He}(e, e'p)pn$ reaction versus missing energy E_m . The vertical arrow gives the peak position expected for disintegration of correlated pairs. The dotted curve presents a PWIA calculation using Salme's spectral function and σ_{cc1} electron-proton off-shell cross section. Other curves are recent theoretical predictions of J. M. Laget from the PWIA (dash dot) to PWIA + FSI (long dash) to full calculation (solid), including meson exchange current and final state interactions. In the 620 MeV/c panel, the additional short dash curve is a calculation with PWIA + FSI only within the correlated pair.

various interaction effects. The calculation is based on a diagrammatic expansion of the reaction amplitude, up to and including two loops [13]. Both single and double NN scattering, as well as meson exchange and Δ formation are included. The bound-state wave function is a solution of the Faddeev equation used by the Hannover group [14] for the Paris potential [15]. The kinematics are relativistic, nucleon and meson propagators are relativistic and no angular approximations (Glauber) have been made in the various loop integrals. At low energies, below NN relative kinetic energy of about 500 MeV, the NN amplitude is the solution of the Lippman-Schwinger equation for the Paris potential. In our experiment, the NN relative kinetic energy is higher ($T_{NN} = 840$ MeV) and the absorptive part of the interaction dominates the NN scattering amplitude - the implementation is explained in [16]. Further details of the model can be found in [17].

We can see from the figure that the cross sections, especially at large p_m , are strongly enhanced by final-state interactions. FSI between the two active nucleons - see Fig. 1b - increase the cross section by a factor of about four. While rescattering between one nucleon in the correlated pair and the third nucleon - see Fig. 1c - might be expected to modify the shape of the distribution, the effects are slight; this is indicated by the additional calculation included in the 620 MeV/c panel of Fig. 2, in which FSI with the spectator nucleon are turned off. Neither the shape nor magnitude of the peak is much affected. MEC effects are small.

Figure 3 shows the effective momentum density distribution, obtained by integrating the theory and cross-section data, such as those shown in Fig. 2, over missing energy from threshold to 140 MeV, as discussed above - see Eq. 2. Uncertainties from missing tails of the 3bbu peak, within this integration range, due to limited experimental acceptance are negligible on the scale of Fig. 3. The 3bbu distribution is not the same shape as the 2bbu distribution from [6]. The 3bbu distribution tends to have a much larger relative strength for high missing momentum, suggesting an important role for correlations.

The relative importance of the underlying processes can be investigated within theories. The PWIA curve includes conventional correlations but not final state interactions. Since the PWIA calculations show an order of magnitude enhancement of the 3bbu over the 2bbu at high missing momentum, we can infer that the relative enhancement of the 3bbu is largely from correlations. Here, the two-body correlations are more clearly seen in 3bbu than in the 2bbu, where the available phase space is reduced since two nucleons are forced to form the deuteron. The differences between the PWIA calculations and the data and full calculations further indicate the greater importance of final-state interactions in the

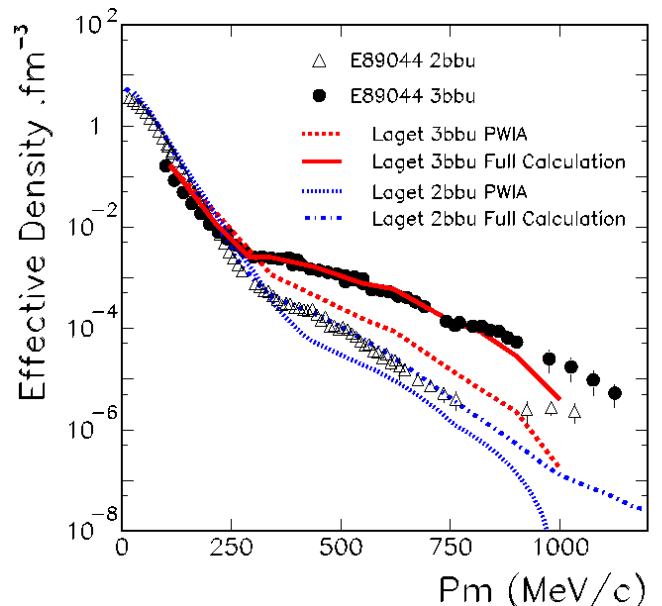


FIG. 3: (color online). Proton effective momentum density distributions in ${}^3\text{He}$ extracted from ${}^3\text{He}(e, e'p)pn$ (filled black circles) and ${}^3\text{He}(e, e'p)d$ (open black triangles), compared to calculations from Laget. The 3bbu integration covers E_M from threshold to 140 MeV.

3bbu. The generally good agreement of the full calculations shown in Figs. 2 and 3 indicates that, at this level of comparison, there is no need for correlations beyond those already present in a modern conventional nuclear physics model.

The conclusions described above might appear to be no longer valid for $p_m \approx 1$ GeV/c. Here the 2bbu distribution flattens out, while the 3bbu distribution continues to fall. This behavior is contrary to what one would expect from the importance of correlations. At these very high p_m , however, one has to be careful about drawing conclusions. The center of the 3bbu correlation peak moves past $E_m = 140$ MeV, outside of the integration range and into the pion production region, at $p_m \approx 800$ MeV/c, as shown in Fig. 2. Thus, the experimental integration is only including a fraction of the 3bbu strength at large p_m , leading to the apparent narrowing of the gap between the 2bbu and 3bbu. Thus, a correction is needed for a more meaningful comparison of 3bbu to 2bbu at large p_m . We have estimated the fraction of the strength missed by our experimental integration by calculating what fraction of the total strength of the Laget full calculation lies in the region $E_m < 140$ MeV. This is only a crude estimate, since a close examination of Fig. 2 shows that the calculation has a tendency to underpredict the cross section for the low E_m tail of the correlation peak. The estimated correction factors for the missing 3bbu

strength are about 1.05, 2, and 20 for $p_m = 600, 800,$ and $1000 \text{ MeV}/c$, respectively. Applying the correction to the 3bbu would cause the distribution to roughly flatten out, starting near $750 \text{ MeV}/c$, at a level nearly two orders of magnitude greater than that of the 2bbu. These observed correction factors also lead to our stopping the calculation at $1 \text{ GeV}/c$; the comparison between data and theory is no longer meaningful when only a small fraction of the tail of the distribution is considered. Given these data along with the theoretical calculations, it remains fair to conclude that the correlations in the wave function preferentially lead to the 3bbu channel, and that the reaction mechanism is reasonably well understood in a modern, conventional nuclear physics model.

In summary, results for the cross section at constant \vec{q} and ω have been presented for the ${}^3\text{He}(e, e'p)pn$ reaction channel. The experimental data are both much higher in statistics and more extensive in kinematic coverage than any previous measurement. Theoretical predictions are in good agreement with the data, leading to the conclusion that the cross section at large missing momenta is strongly enhanced by nucleon-nucleon correlations, with additional enhancement from final-state interactions. Rescattering of one of the correlated nucleons with the third (spectator) nucleon is small and does not affect this conclusion. Since the conventional NN correlations present in a modern nuclear wave function appear sufficient to explain the data, there is no strong indication of a need to include any additional exotic physics. Separated response functions, which are possible with data from the other kinematics of this experiment, will provide us with more complete tests of the theoretical models.

We acknowledge the outstanding support of the staff of the Accelerator and Physics Divisions at JLab that made this experiment successful. This work was supported in part by the U.S. Department of Energy contract DE-AC05-84ER40150 under which the Southeastern Universities Research Association (SURA) operates

the Thomas Jefferson National Accelerator Facility, other Department of Energy contracts, the National Science Foundation, the Italian Istituto Nazionale di Fisica Nucleare (INFN), the French Atomic Energy Commission and National Center of Scientific Research, the Natural Sciences and Engineering Research Council of Canada, and Grant-in-Aid for Scientific Research (KAKENHI) (No. 14540239) from the Japan Society for Promotion of Science (JSPS).

-
- [1] L. Frankfurt and M. Strikman, Phys. Rep. **76**, 236 (1981).
 - [2] J. M. Laget, Nucl. Phys. A **358**, 275 (1981).
 - [3] C. Marchand *et al.*, Phys. Rev. Lett. **60**, 1703 (1988).
 - [4] T. DeForest, Nucl. Phys. A **392**, 232 (1983).
 - [5] Jefferson Lab Experiment E89-044, *Selected Studies of the ${}^3\text{He}$ nucleus through electrodisintegration at High Momentum Transfer*, M. Epstein, A. Saha, and E. Voutier, spokespeople.
 - [6] M. Rvachev *et al.*, submitted to Phys. Rev. Lett., and Ph.D. thesis, Massachusetts Institute of Technology (2003).
 - [7] J. Alcorn *et al.*, Nucl. Inst. Meth. A **522**, 294 (2004); see also <http://hallaweb.jlab.org/equipment/HRS.html>.
 - [8] A. Amroun *et al.*, Nucl. Phys. A **579**, 596 (1994).
 - [9] See <http://www.physics.odu.edu/~ulmer/mceep/mceep.html>.
 - [10] E. Borie and D. Drechsel, Nucl. Phys. A **167**, 369 (1971).
 - [11] A. Kievsky, E. Pace, G. Salme and M. Viviani, Phys. Rev. C **56**, 64 (1997).
 - [12] J. M. Laget, Phys. Lett. B **151**, 325 (1985).
 - [13] J. M. Laget, Phys. Rep. **69**, 1 (1981).
 - [14] C. Hadjuk *et al.*, Nucl. Phys. A **369**, 321 (1981), and Nucl. Phys. A **405**, 581 (1983).
 - [15] M. Lacombe *et al.*, Phys. Lett. B **101**, 139 (1981).
 - [16] J. M. Laget, Few Body Syst. Supp. **15**, 171 (2003), and J. M. Laget, submitted for publication and arxiv:nucl-th/0407072.
 - [17] J. M. Laget, Nucl. Phys. A **579**, 333 (1994).